CrossMark

ORIGINAL RESEARCH PAPER

Array-derived rotational seismic motions: revisited

Alberto Castellani[1]

Abstract Rotation motions derived from measurements collected by arrays of translation accelerometers are investigated. The procedure is applicable to the rotation around any one axis, however in the paper rotations around a horizontal axis, i.e. rotations in a vertical plane, are focused. Since the early training of the arrays, the spatial distribution of the translation acceleration has been described through the cross power spectrum of acceler- ations at nearby stations (Harichandran in Workshop on spatial variation of earthquake ground motion 1988, structural safety, 1991; Evans et al. in Workshop on rotational ground motion, Menlo Park, 2006; Abrahamson in Estimation of seismic wave coherency and rupture velocity using the SMART 1 strong—motion array recordings, 1985). These cross spectra can be used to derive rotation components of the seismic motion (Castellani et al. in Earthq Eng Struct Dyn 41:875–891, 2012. doi:10.1002/eqe.1163; Castellani and Zembaty in Eng Struct 18(8):597–603, 1996). In recent times the evaluation of the rotation at a point has been attempted through apposite instruments. Rotation records concerning earthquakes observed at a single station in Taiwan, and rotations obtained from cross spectra have shown a satisfactory agreement (Castellani et al. in Earthq Eng Struct Dyn 41:875–891, 2012. doi:10.1002/eqe.1163), when properly normalized. In the present paper, the set of records collected at a dense array of acceleration recorders are represented through an interpolation function of the surface coordinates of the instruments. In this way rotation is measured as a function of space and time, free from any model of propagation. Propagation models hold in fact at some distance from the source, in particular at distances where the source mechanism can be represented as a point source. The proposed procedure is quite general, but the present application is limited to the sets of records available to the author: the records collected at seven stations SMART-1 in Lotung, Taiwan, one event of January 29, 1981, and another of 1986 (all elaborations here shown refer to the latter one). The seven stations are nearly aligned along a precise axis Fig. 2, and the time correlations between the records at different stations is perceptible. An apparent limit of the procedure

✉ Alberto Castellani
  alberto.castellani@polimi.it

[1] Politecnico di Milano, piazza Leonardo da Vinci 32, 20133 Milan, Italy

is given by the dispersion of the acceleration amplitude at the stations. Kawakami and Sharma (Earthq Eng Struct Dyn 28:1273–1294, 1999) have examined the spatial variation of acceleration response spectra using the entire set of strong motion records SMART-1. This spatial dispersion is repetitively present in records of closely spaced arrays, and it is responsible itself of rotations. As a consequence, in presence of such variability, the entire set of records of the array would be suitable. The way the interpolation function is determined in function of the coordinates is dictated by two requirements: (1) fitting, and (2) smoothing. Fitting requires that at least the records collected at positions at hundred meters distance (C00, I03 and I12 in Fig. 2) shall be reproduced correctly. The smoothing is attempted by suitably truncating the series to the first terms, see Sect. 3. The power spectrum of the signal shows that the dominant frequencies for rotation are in the range of 3–11 cps. Excitation provided by rotation may thus be meaningful for chimneys, tall buildings, and bridges. Underground tubes are sensitive to excitations at quasi-static frequency.

Keywords Rotational seismology · Rotational strong ground motion · Rotational transducers · Rotations in structural response · Multivariate linear regression

1 Introduction

In front of the number of theoretical and numerical approaches that have been proposed, rotational ground motions have not been observed directly until the last decade due to the lack of appropriate instruments. The direct measurement of point rotations has been attempted through "ad hoc" designed devices, sensitive to torsion as tilt-meter, ring lasers and broadband rotation meters (Kalkan and Grazier 2007; Takeo 1998; Igel et al. 2007; Spudich et al. 1995; Zhang et al. 2004; Liu et al. 2009; Spudich and Fletcher 2009; Jaroszewicz et al. 2012; Lee and Liang 2008; Geological Survey Open-File Report 2007). However such devices are not in common use, and suitable applications in earthquake engineering are still rare and an open-challenging task.

   Valid progress in the knowledge of the spatial distribution has been achieved through statistical studies (Kawakami and Sharma 1999; Lee and Trifunac 2009; Lavallée and Archuleta 2003; Zerva and Zhang 1997). A well organized state-of-the-art of the different facets of rotational seismology, concerning theoretical investigations, instrumentation, analysis of ground motion observations and engineering applications is provided by Lee et al., in an introductive paper of Bulletin of Seismological Society of America (Geological Survey Open-File Report 2007) and by Todorovska et al. (2008). It is worth to remember that in the application of Lee and Trifunac (2009), both average and point rotations should to be considered at the same time, for proper formulation of dynamic response of discrete systems.

   Measurements in the near-field of earthquakes in Japan, Takeo (1998) indicate that rotational ground motions may be many times larger than expected from classical elasticity theory based on a propagation model. Direct observations have been published, Igel et al. (2005), Igel et al. (2007), Spudich et al. (1995), Zhang et al. (2004), Shabestari and Yamazaki (2003), and in particular Liu et al. (2009), Fig. 1.

   Data presented by Liu et al. (2009), concerning 52 earthquake records collected at a single station in Taiwan, are presented in Fig. 1. The PRV is the maximum among the

Fig. 1 Elaboration of data presented by (Liu et al. (2009). Ratio between the peak rotation velocity PRV and the peak horizontal acceleration PGA, in mrad × s/m. Average value 1.43
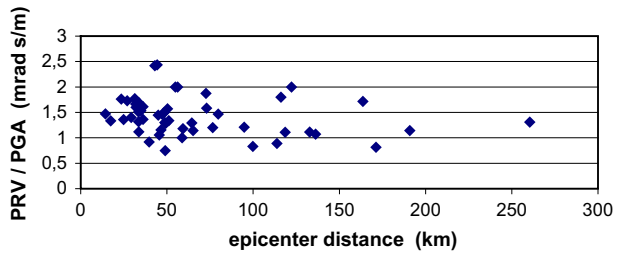
three components, and the PGA is the maximum between the two horizontal components. The ratio is shown in function of the distance from epicentre. The same ratio, computed according to array-derived cross spectra of accelerations (Castellani et al. 2012), is in good agreement with the average value of these data.

Statistical estimate from the set of data of Fig. 1 does not identify a marked dependence of the ratio on the distance from epicentre. Meanwhile, no one record is referring to a distance equal or less to the focal depth, and only 18 to a distance less than 1.5 the focal depth. Consistently, this amount of data, which is the richest so far available, does not provide a clear information for the recurrent conjecture that in the near field rotations might be higher, for the same peak horizontal acceleration (Stupazzini et al. 2009; Takeo 1998).

The paper mentions much higher amplitudes for the two horizontal components of the translation than that for the vertical component, everywhere mention is explicit. This circumstance is generally characteristic of medium to far region. For a same PGA, if for PRV only rotations in a vertical plane is considered, the dependence on distance would be more pronounced.

A direct observation of ground rotations caused by the M = 6.0, 2004 Parkfield earthquake and aftershocks has been published by Spudich and Fletcher (2009). The paper is mainly devoted to the mathematical process to ascertain reliable values for rotations. Results are not in a format suitable for a direct comparison to those of Fig. 1, however the order of magnitude of rotation rate is respected.

Array-derived rotations, and direct measurements at single points, are in principle a parent experimental measure, being the punctual rotation equal to the derivative, with respect to space, of the translations. One weakness of the array-derived rotations, that of being sensitive to "noise", is likely to be present in point rotation instruments as well. In any case, the practical application dealt with in a previous study (Castellani et al. 2012), has shown that the high frequency content of the rotation motion has little impact on civil engineering structures. On the other hand, excitation provided by rotation in the frequency range 1–5 cps, may be meaningful for tall buildings (Di Cesare et al. 2014; Castellani et al. 2012), chimneys (Castellani and Zembaty 1996), and bridges. Underground tubes are sensitive to excitations at quasi-static frequency. For this application, strains have been computed by Paolucci and Smerzini (2008).

A comparison between rotations from dense-arrays and point measurements, during the same event, and at the same location, has been provided for the first time by Suryanto et al. (2006). The overall fit is estimated to be satisfactory, although factors of 2–5 between such measures have been observed. Authors explain them in terms of local site conditions.

A comparison of rotational waveforms generated by point rotation measurement to those derived from a translational array has been made by Lin et al. (2012). It is of interest

both for testing the performance of the rotational sensor and evaluating the rotational motions derived from measurements by arrays of translational seismometers.

2 Representation of the ground motion

In a Cartesian space, let X, Y, and Z be the orientation axes, the latter being vertical. Along these axes the acceleration components during a ground motion are $u(t)$, $v(t)$, and $w(t)$. In the following the attention is focused on the vertical $w(t)$ acceleration, but the elaboration to follow can be applied to each of the three space components.

The set of records will be represented through an interpolation function,

$$w(t,x,y) = d_1(t) + d_2(t)x + d_3(t)x^2 + d_4(t)y + d_5(t)xy \tag{1}$$

where x and y are the coordinates, and d_1, d_2, ..., d_5 are unknown functions of time, to be computed instant by instant. If the interpolation function is reliable enough, it is possible to evaluate rotations, and shear strains, deriving Eq. 1 with respect to the spatial coordinates.

The quantities d_1, d_2, ... are obtained by solving at each instant of time the system of equations,

$$w_k(t) = d_1(t) + d_2(t)x_k + d_3(t)x_k^2 + d_4(t)y_k + d_5(t)x_ky_k \tag{2}$$

where $w_k(t)$ is the vertical acceleration recorded at the k-instrument, k = 1, 2, …, N, N being the number of instruments.

The procedure to obtain d_1, d_2, ... is explained in the next paragraph. It is repeated instant by instant, independently from an instant to the other. An important worth of the procedure is to find out rotations as continuous functions of time.

Continuum mechanics defines rotations of the elementary volume around the Y-axis, ψ_y:

$$\psi_y = \frac{1}{2}\left(\frac{\partial w}{\partial x} - \frac{\partial u}{\partial z}\right) \tag{3}$$

and shear strain γ_{xz} as:

$$\gamma_{xz} = \frac{1}{2}\left(\frac{\partial w}{\partial x} + \frac{\partial u}{\partial z}\right) \tag{4}$$

These quantities for a soil deposit under earthquake excitation are considered. The free surface condition at the top of the deposit implies that the shear strain γ_{xz} is equal to zero: therefore the rotation along the free surface is given, equivalently, by:

$$\psi_y = \frac{\partial w}{\partial x}, \quad \text{or} \quad \psi_y = -\frac{\partial u}{\partial z} \tag{5a, 5b}$$

This quantity for a soil deposit acted by an earthquake excitation is considered.

The dense array of earthquake motion recorders in Taiwan is composed by N = 29 instruments, i.e., k = 1, 2, …, 29. In our hope all records collected in some seismic events (Fig. 2) will be utilized to build up $w(t, x, y)$. However only seven records are available up to now to the present Author.

The way the function $w(t, x, y)$ is determined in function of the coordinates is dictated by two requirements: (1) fitting, and (2) smoothing.

The fitting is solved in the least square sense over the set of records, as it will be explained in the following. Fitting requires that at least the records collected at positions at hundreds meter distance (C00, I03 and I06) should be reproduced correctly. Fitting is tested for the entire time history. For testifying the good performance only a short time windows is offered, Figs. 4 and 5, where the inaccuracy is of the order of a few percent.

The smoothing is attempted by truncating the series (1) to the first five terms. In theory the series could be of seven terms being available seven stations and thus seven equations for seven unknowns. The analytical functions so determined would be more irregular than expected, because higher terms are likely to introduce spurious effects that might affect the representation between station and station. In the present case the limited amount of accelerograms available, $N = 7$, has obliged to limit the unknowns to 5. This condition establishes the need to have available a higher number of records.

The first 1500 time accelerations have been considered, for $t = 0...15$ s, a common time scale for all stations. If it where only for the terms of first order (in x, y), the rotation, instant by instant would be the same along the entire region. The space dependence (Eq. 1), is such that rotation and its first order dependence on coordinates can be inferred.

Observing the records of the seven stations for which records are available, a component of propagation along the X axis may be suggested, as may be seen by observing carefully the peaks in Fig. 3.

3 Interpolating function

For each instant of time, Eq. (2) can be written in matrix form:

$$\mathbf{w} = \mathbf{A} \cdot \mathbf{d} \qquad (6)$$

where $\mathbf{A}$ is the matrix of coefficients, given by the coordinates of the stations,

$$\mathbf{A} = \begin{vmatrix} 1 & x_1 & x_1^2 & y_1 & x_1 \times y_1 \\ 1 & x_2 & x_2^2 & y_2 & x_2 \times y_2 \\ ... & ... & ... & ... & ... \\ ... & x_7 & x_7^2 & y_7 & x_7 \times y_7 \end{vmatrix}$$

$x_1\, y_1$ are the surface coordinates of the station C00,
$x_2\, y_2$ are those of I12,
....
$x_7\, y_7$ are those of the station O07,
$\mathbf{w}(t)$ is the column vector of the measured accelerations,
$w_1(t) = w(C00, t)$,
$w_2(t) = w(I12, t)$,
$w_3(t) = w(I06, t)$,
$w_4(t) = w(M01, t)$,
$w_5(t) = w(M07, t)$,
$w_6(t) = w(O1, t)$,
$w_7(t) = w(O7, t)$.
$\mathbf{d}$ is the column vector of the five unknown, and the dotted point $\cdot$ denotes the product of the matrix to the column vector $\mathbf{d}$.

The coefficients of "best fit", $d_1\, d_2, ..., d_5$ ... are function of the instant of time t. There are more equations, 7, than unknowns, 5. The best fit is sought, the one which comes

closest to satisfying all equations simultaneously. If closeness is defined in the least square sense, i.e. that to sum of the squares of the differences between the left and the right-hand side of Eq. (2) be minimized, then the over-determined linear problem reduces to a usually solvable linear problem, called the linear least-square problem.

The reduced set of equations to be solved can be written as the set of 5×5 equations:

$$\left(\mathbf{A}^{\mathrm{T}} \, \mathbf{A}\right) \cdot \mathbf{d} = \left(\mathbf{A}^{\mathrm{T}} \cdot \mathrm{w}\right) \tag{7}$$

where $\mathbf{A}^{\mathrm{T}}$ denotes the transpose of the matrix $\mathbf{A}$, and the dotted point $\cdot$ denotes the product of the matrix to the column vector $\mathbf{d}$ or $\mathbf{w}.$

The paper shows that the procedure can be valid, meanwhile a larger number of records is necessary to reach more reliable data about rotations, as already said (Fig. 2).

4 Some results: fitting

In Fig. 3 the vertical acceleration at given points is shown. Some time correlation is noticeable. However there is a systematic larger amplitude at the station M01 with respect to the other stations. A similar condition applies for the other stations, i.e. time correlation
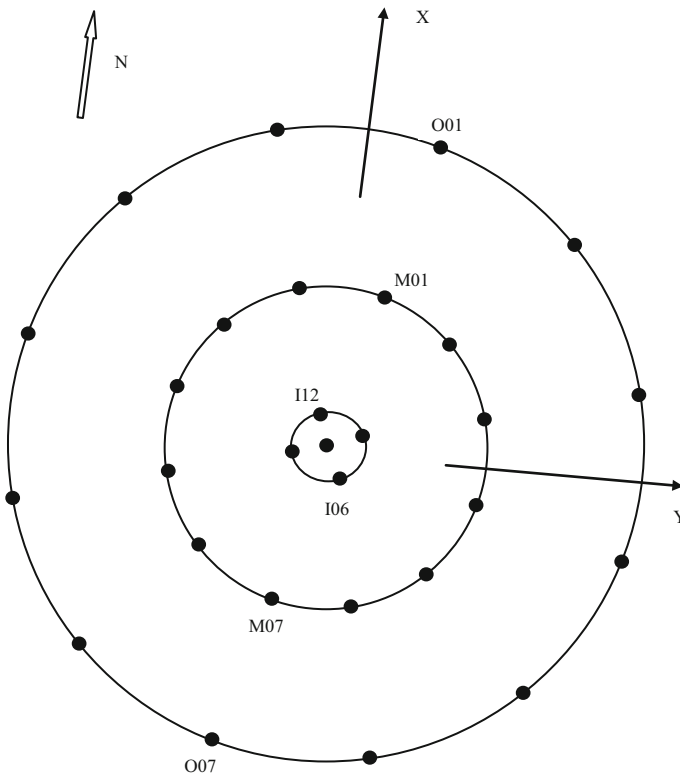

Fig. 2 Stations of the Taiwan dense array of instruments. Named are the seven stations for which records are available to the Author, events of 1981 and 1986. The central station is named C00. Radius of the inner circus is 100 m, that of the intermediate one is 500 m, and that of the outer one is 1000 m
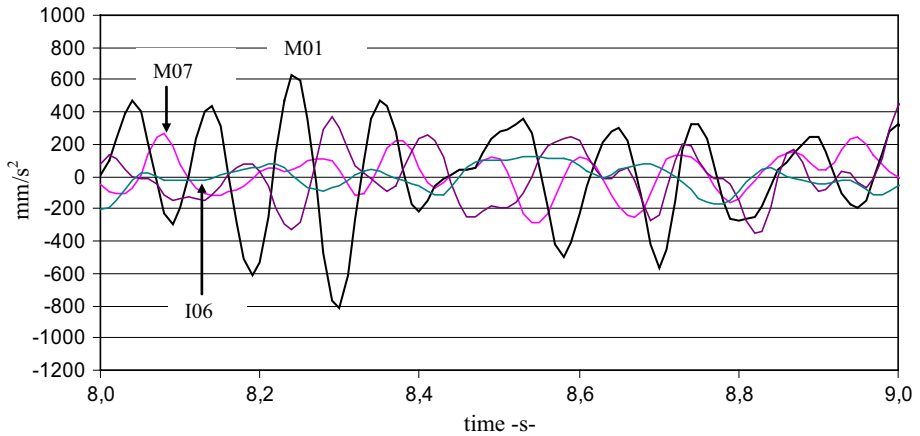
Fig. 3 Time window between 8 and 9 s, stations M01, M07 and I06. In the ordinate, vertical acceleration in mm/s^2. Some time correlation is noticeable. However there is a systematic larger amplitude at the station M01 with respect to the other stations

is visible, and the amplitude is rather different. Table 1 reports the peaks of the records, that range from 277 to 831 mm/s^2.

The fitting requirement is respected for the stations I12 and I06, Figs. 4 and 5. A short time window is shown, of 2 s duration. However the quality of fitting is similar for the entire time duration. Less satisfying agreement is remarked for the central station C00, where the time evolution is respected, i.e. the time position of all peaks are respected, but the ordinates of the accelerations built according to the interpolation procedure are around 80 % of the original ones.

For the central station this is because the interpolation procedure depends also on the variability of the amplitude, which should be recognized as rather random. If we derive rotations by the differences from one another record, the ratio PRV/PGA, reported in Fig. 1, will be random itself. The quality of the interpolation relies thus on the number of equations that it involves. The fitting requirement is even less respected for the more distant stations.

The procedure implied by Eq. 7 ignores the time correlation because the 5 × 5 equations are solved independently instant by instant. However, as it will be seen, rotations appear to be continuous functions of time, and the time correlation present in the original data is kept in the rotations, Fig. 6.

Table 1 Peak vertical acceleration at the stations, during the entire time history	**Station**	**Absolute peak (mm/s^2)**

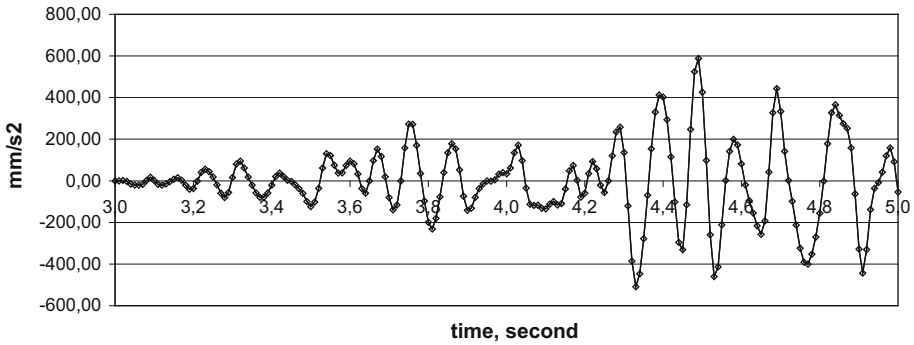| Station	Absolute peak (mm/s^2)
C00	415.98
I06	313.25
I12	589.18
M07	494.84
M01	831.70
O07	277.04
O01	292.20

Fig. 4 Time window of the vertical acceleration at station I12. In continuous line the original function. By small squares the function built up by the present procedure, Eq. 7
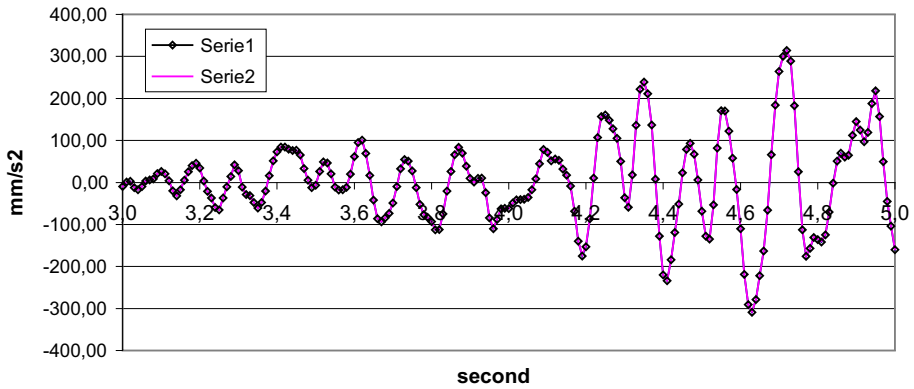

Fig. 5 Time window of the vertical acceleration at station I06. In continuous line the original function. By small squares the function built up from the present procedure, Eq. 7

5 Rotations

Rotations around the stations I06 and I12 are investigated, for which the representation of the vertical acceleration $w(t)$ is reliable (Fig. 7). Rotation is measured through the expression in Eq. 5a. Figures 8 and 9 allows a more detailed view of the two rotations.

The main frequency of both signals is around 8.2 cps (cycles per second). Figure 6 is the picture of both acceleration rotations. Figures 8 and 9 show a correlation between the two signals, with a time lag of approximately 0.058 s. The time lag between peaks at a same station is 0.11 s, in substantial agreement with the peak of the power spectrum, discussed later on. Again the amplitude of signal at station I12 is higher than that at station I06.

6 Power spectrum of rotation accelerations

There are more functions under the name of power spectrum. In the following, the soil rotation is firstly transformed in Fourier series, in the standard way:
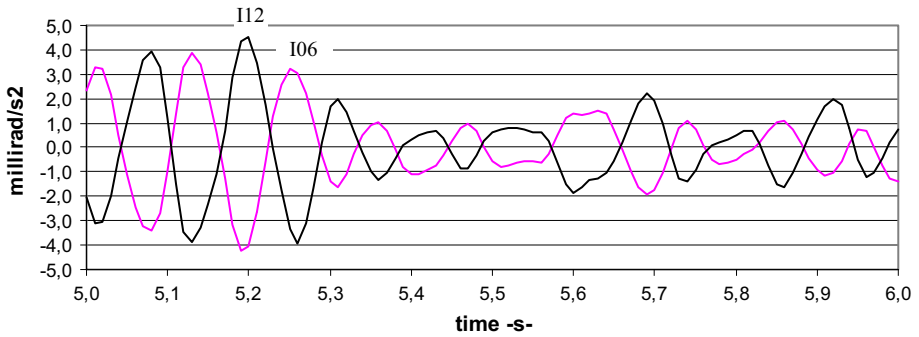
Fig. 6 Stations I06 and I12. Window of the time history of rotation accelerations, between 5 and 6 s
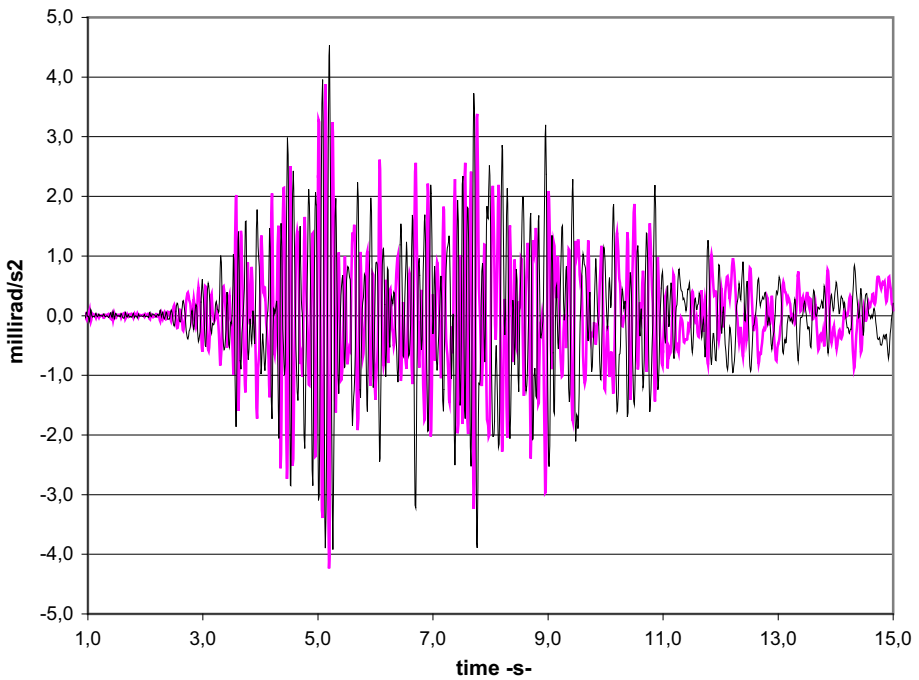

Fig. 7 Entire time history of rotation accelerations, in mrad/s^2, at the two stations

$$w(t) = a_1 \cos(w_1 \times t + \varphi_1) + a_2 \cos(w_2 \times t + \varphi_2) + \cdots + a_i \cos(w_i \times t + \varphi_i) + \cdots$$
$$+ a_N \cos(w_n \times t + \varphi_n); \tag{8}$$

where t is time in seconds, $\omega_1 = \frac{2\pi}{T}$ rad/s, where T is the duration of record, $\omega_2 = 2 \times \omega_1, \ldots, \omega_i = i \times \omega_1, \ldots, \omega_n = n \times \omega_1$, $a_i = \sqrt{b_i^2 + c_i^2}$ with $b_i = \frac{1}{\pi} \int_0^T w(t) \times \cos(\omega_i t)$ dt; $c_i = \frac{1}{\pi} \int_0^T w(t) \times \sin(\omega_i t) \, dt$, φ_i are phases, with $\varphi_i = a \tan\left(\frac{c_i}{b_i}\right)$.
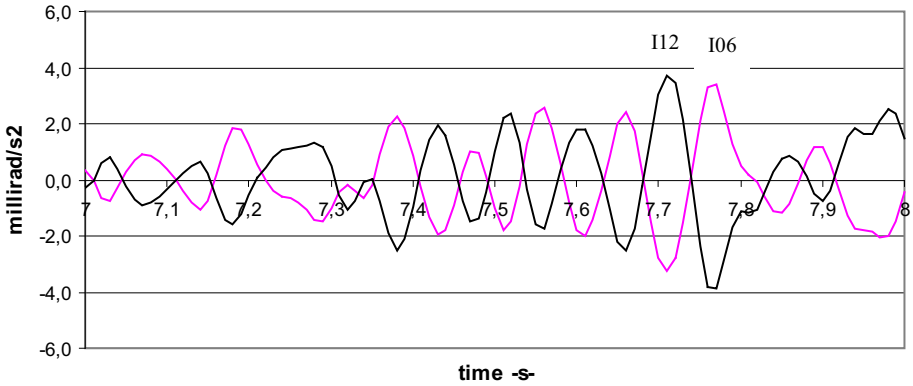
Fig. 8 Window of the time history of rotation accelerations, between 7 and 8 s. The average time lag between the peaks of one and the other station is 0.058 s. The time lag between peaks at a same station is 0.11 s
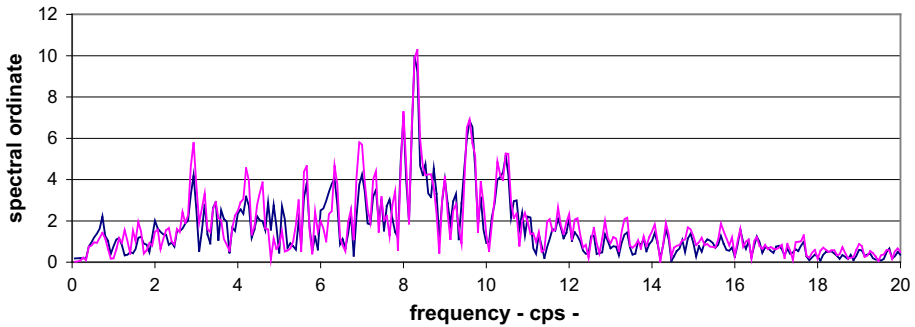

Fig. 9 Power-spectrum of rotation acceleration, at stations I06 and I12. Again the spectrum at I112 is higher that that at I06. However the highest peak is located at a same frequency of 8.3 cps and shows a similar amplitude of the two spectra

Given the input signal as a Fourier series, the power-spectrum is:

$$S_w(\omega_i) = \left(\frac{a_i}{1/T}\right) \qquad (9)$$

Notice that in the literature the same quantity is alternatively expressed as:

$$S_w(\omega_i) = \left(\frac{a_i^2}{1/T}\right) \qquad (10)$$

In the present formulation the spectral ordinate is in $(mrad/s^2)/cps$ units. In all formulations, the power-spectrum is suitable to identify the range of frequencies where the signal is meaningful. Figure 10 shows that the soil rotation so far computed are meaningful in the range 4–11 cps, and the peak is at around 8.5 cps, consistent with the time lag between peaks at a same station, remarked in Fig. 8. It confirms that the soil rotation may constitute an important component of the seismic motion for some construction. In the papers (Di
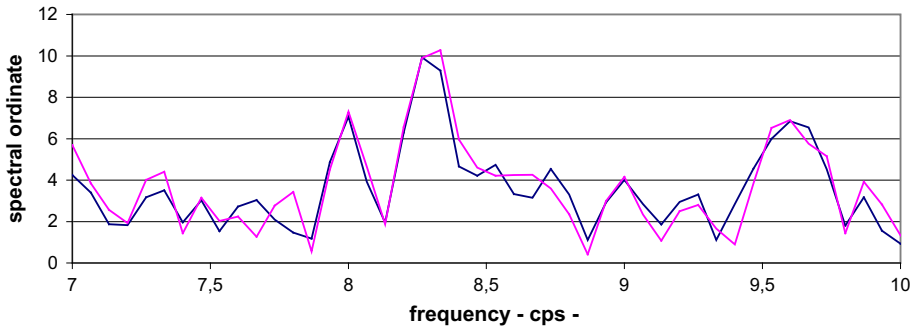
Fig. 10 Detail of the power-spectrum of rotation acceleration, at stations I06 and I12

Cesare et al. 2014; Yin et al. 2016) and in previous studies (Castellani et al. 2012; Castellani and Zembaty 1996), the problem has been attempted on how much this signal is effective with respect to the excitation provided by translation motion.

7 Comparison with other results, and conclusions

Figure 1 presented data by Liu et al. (2009), on the basis of the ratio between the peak rotation velocity PRV, and the peak horizontal acceleration PGA, in mrad × s/m. Average value 1.43.

The picture concerns 52 earthquake records collected at a single station in Taiwan. The PRV is the maximum among the three components, and the PGA is the maximum between the two horizontal components. The ratio is shown in function of the distance from epi-centre. The same ratio, computed according to rotations obtained from cross spectra of array-derived accelerations, is in good agreement with the average value of these data (Castellani et al. 2012), Table 2.

In the present evaluation the same ratio is between 0.11 and 0.216, i.e. from 5 to 10 times less than the same ratio in Fig. 1. There are more reasons that justify why this procedure has led to a lesser ratio PRV/PGA.

Table 2 PRV/PGA reported in Castellani et al. (2012)

Earthquake	Ep. dist. (km)	PRV (mrad/s)	PGA (m/s^2)	PRV/PGA [(mrad s)/m]
SMART-1(5): C00	30.31	1.265	1.102	1.15
SMART-1(5): O07	28.96	0.946	0.798	1.19
SMART-1(5): O01	31.99	1.296	0.997	1.30
SMART-1(33): C00	44.93	0.913	0.636	1.43
SMART-1(33): O07	44.73	0.634	0.517	1.23
SMART-1(33): O01	45.10	0.691	0.569	1.22
SMART-1(33): M07	44.95	1.054	0.690	1.53
SMART-1(33): I01	44.94	1.563	1.085	1.44

1. There is a sensible scatter between the amplitude of acceleration records, as shown in Table 1. This establish the need to have available a larger set of records, for a suitable application of the least square procedure, Eq. 7, as already remarked.
2. The direction of propagation, implied by the line around which station are aligned in Fig. 2, is some how arbitrary. It allows to observe the rotation in the plane XZ and it forces to disregard the rotation in the perpendicular plane YZ.
3. In the Liu et al. paper, the PRV is the maximum among the three components. In the present application PRV in a vertical plane is considered, and besides in one precise plane. The vertical accelerations are in general less ample than the two horizontal components, and thus, for a same PGA, rotations in a vertical plane are less than the corresponding one in the horizontal plane.
4. In the general case, rotations are provided as well by the local and neighboring topographic effects. In this elaboration they are absent.

Under these premises, the interpolation of the array-derived records may be proposed as a promising tool to elaborate rotations, free from assumptions on a propagation model.

References

Abrahamson NA (1985) Estimation of seismic wave coherency and rupture velocity using the SMART 1 strong—motion array recordings. Report no. UBC/EERC—85/02, March 1985

Castellani A, Zembaty Z (1996) Comparison between earthquake rotation spectra obtained by different experimental sources. Eng Struct 18(8):597–603

Castellani A, Stupazzini M, Guidotti R (2012) Free-field rotations during earthquakes: relevance on buildings. Earthq Eng Struct Dyn 41:875–891. Published online 21 September 2011 in Wiley Online Library (wileyonlinelibrary.com). doi:10.1002/eqe.1163

Di Cesare A, Ponzo FC, Vona M, Dolce M, Masi A, Gallipoli MR, Mucciarelli M (2014) Identification of the structural model and analysis of the global seismic behaviour of a RC damaged building. Soil Dyn Earthq Eng 65:131–141

Evans JR, Graizer V, Huang B-S, Hudnut KW, Hutt CR, Lee WHK, Liu C-C, Nigbor R, Safak E, Savage WU, Trifunac M, Wu C-F (2006) Workshop on rotational ground motion, held in Menlo Park on 16 February 2006

Harichandran RS (1991) Estimating the spatial variation of earthquake ground motion from dense array recordings. Workshop on spatial variation of earthquake ground motion 1988, structural safety, vol 10, 1–3 May 1991

Igel H, Schreiber KU, Flaws A, Schuberth B, Velikoseltsev A, Cochard A (2005) Rotational motions induced by the M8. 1 Tokachi-oki earthquake, September 25, 2003. Geophys Res Lett 32(8):L08309. doi:10.1029/2004GL022336

Igel H, Cochard A, Wassermann J, Flaws A, Schreiber U, Velikoseltsev A, Pham Dim N (2007) Broad-band observations of earthquake-induced rotational ground motions. Geophys J Int 168:182–196

Jaroszewicz LR, Krajewski Z, Teisseyre KP (2012) Fibre-optic Sagnac interferometer as seismograph for direct monitoring of rotational events, earthquake research and analysis—statistical studies, observations and planning. In: D'Amico S (ed) In Tech. Available from http://www.intechopen.com/books/earthquake-research-and-analysis-statisticalstudies-observations-and-planning/fibre-optic-sagnac-interferometer-as-the-seismograph-for-directmonitoring-of-the-rotational-phenomena. ISBN: 978-953-51-0134-5

Kalkan E, Grazier V (2007) Multicomponent ground motion response spectra for coupled horizontal, vertical, angular accelerations, and tilt. J Earthq Technol 44(1):259–284

Kawakami H, Sharma S (1999) Statistical study of spatial variation of response spectrum using free field records of dense strong motion arrays. Earthq Eng Struct Dyn 28:1273–1294

Lavallée D, Archuleta RJ (2003) Stochastic modeling of slip spatial complexities for the 1979 Imperial Valley, California, earthquake. Geophys Res Lett 30(5):1245

Lee VW, Liang J (2008) Rotational components of strong-motion earthquakes. 14th world conference on earthquake engineering, October 12–17, Beijing, China

Lee VW, Trifunac MD (2009) Empirical scaling of rotational spectra of strong earthquake ground motion. Bull Seismol Soc Am 99(2B):1378–1390

Lin Chin-Jen, Huang Wen-Gee, Huang Han-Pang, Huang Bor-Shouh, Chin-Shang Ku, Liu Chun-Chi (2012) Investigation of array-derived rotation in TAIPEI 101. J Seismol 16:721–731. doi:10.1007/s10950-012-9306-7

Liu C-C, Huang B-S, Lee WHK, Lin C-J (2009) Observing rotational and translational ground motions at the HGSD station in taiwan from 2004 to 2008. Bull Seismol Soc Am 99(2B):1228–1236

Paolucci R, Smerzini C (2008) Earthquake induced transient ground strain from dense seismic networks. Earthq Spectra 24(2):453–470

Shabestari KT, Yamazaki F (2003) Near-fault spatial variation in strong ground motion due to rupture directivity and hanging wall effects from the Chi-Chi, Taiwan earthquake. Earthq Eng Struct Dyn 32:2197–2219

Spudich P, Fletcher JB (2009) Observation and prediction of dynamic ground strains, tilts and torsions caused by the M6.0 2004 Parkfield, California, earthquake and aftershocks derived from UPSAR array observations. Bull Seismol Soc Am 98:1898–1914

Spudich P, Steck LK, Hellweg M, Fletcher JB, Baker LM (1995) Transient stresses at Parkfield, California, produced by the M 7.4 earthquake of June 28, 1992: observations from the UPSAR dense seismograph array. J Geophys Res 100(B1):675–690

Stupazzini M, De La Puente J, Smerzini C, Kaeser M, Castellani A, Igel H (2009) Study of rotational ground motion in the near field region. Bull Seismol Soc Am 99(2B):1271–1286

Suryanto W, Igel H, Cochard A, Shuberth B, Vollmer D, Scherbaum F, Schreiber U, Velikoseltsev A (2006) First comparison of array-derived rotational ground motions with direct ring laser measurements. Bull Seismol Soc Am 96(6):2059–2071

Takeo M (1998) Ground rotational motions recorded in near-source region of earthquakes. Geophys Res Lett 25:789–792

Todorovska MI, Igel H, Trifunac MD, Lee WHK (2008) Rotational earthquake motions—international working group and its activities. The 14th world conference on earthquake engineering, 12–17 October 2008, Beijing, China

U.S. Geological Survey Open-File Report 2007–1144 (2007) Rotational seismology and engineering applications—Online proceedings for the first international workshop Menlo Park, California, USA, September 18–19, 2007, Compiled and Edited by Lee WHK, Çelebi M, Todorovska MI, Diggles MF

Yin J, Nigbor RL, Chen Q, Steidl J (2016) Engineering analysis of measured rotational ground motion at GVDA. Soil Dyn Earthq Eng 87:125–137

Zerva A, Zhang O (1997) Correlation patterns in characteristics of spatially variable seismic ground motions. Earthquake Eng Struct Dynam 26:19–39

Zhang Y, Xiang-Chu Yin, Peng K (2004) Spatial and temporal variation of LURR and its implication for the tendency of earthquake occurrence in Southern California. Pure appl Geophys 161:2359–2367